Published in final edited form as:
Nat Commun. 2012 ; 3: 1246. doi:10.1038/ncomms2250.

Synaptic tagging and capture in the living rat

K. L. Shires[#], **B. M. da Silva**, **J. P. Hawthorne**, **R. G. M. Morris**, and **S. J. Martin**[*]
University of Edinburgh, Centre for Cognitive and Neural Systems (CCNS), 1 George Square, Edinburgh, EH8 9JZ.

Abstract

In isolated hippocampal slices, decaying long-term potentiation (LTP) can be stabilized, and converted to late-LTP lasting many hours, by prior or subsequent strong high-frequency tetanization of an independent input to a common population of neurons—a phenomenon known as 'synaptic tagging and capture'. Here we show that the same phenomenon occurs in the intact rat. Late-LTP can be induced in CA1 during the inhibition of protein synthesis if an independent input is strongly tetanized beforehand. Conversely, declining early-LTP induced by weak tetanization can be converted into lasting late-LTP by subsequent strong tetanization of a separate input. These findings indicate that synaptic tagging and capture is not limited to *in vitro* preparations; the past and future activity of neurons plays a critical role in determining the persistence of synaptic changes in the living animal, thus providing a bridge between cellular studies of protein-synthesis-dependent synaptic potentiation and behavioural studies of memory persistence.

Keywords

hippocampus; CA1; long-term potentiation; synaptic plasticity; protein synthesis; memory

Introduction

Throughout the history of neuroscience, discoveries about brain function made in both humans and living animals have triggered research into circuit-level, neuronal, and molecular mechanisms. For example, the *in vivo* discovery of long-term potentiation (LTP) of synaptic strength initiated an explosion of interest in the cellular and molecular mechanisms of synaptic change[1]. Similarly, ocular dominance plasticity was observed almost six decades ago in the cortex of the living cat[2], triggering computational models[3] and experimental studies *in vitro* to reveal its physiological basis[4]. The converse is also true; new discoveries at the molecular and cellular level, often in reduced preparations, have led to insights concerning the functioning of the intact nervous system. Examples include classical studies of neuronal plasticity in *Aplysia*[5], the *in vitro* discovery of the homeostatic scaling of synaptic weights[6], and adult neurogenesis[7]. This interdisciplinary interplay between different levels of analysis is both an exciting feature of contemporary neuroscience and a necessary step towards an integrated functional and mechanistic account of the operation of the brain. Although it is generally naïve to explain complex processes such as

[*]Corresponding author.
[#]Current address: Brain Repair Group, Cardiff School of Biosciences, Biomedical Sciences Building, Museum Avenue, Cardiff, CF10 3AX.

Author Contributions K.L.S., B.M.daS., R.G.M.M., and S.J.M. designed the study. K.L.S., B.M.daS., J.P.H., and S.J.M. conducted the experiments and analysed the data. K.L.S., B.M.daS., R.G.M.M., and S.J.M. wrote the manuscript.

Competing financial interests: The authors declare no competing financial interests.

Europe PMC Funders Author Manuscripts

vision or memory with reference only to molecular mechanisms, there may be instances in which cellular processes place such rigid constraints on systems-level properties that the gap between levels can be bridged to realise a full understanding.

For example, the encoding of memory traces in the mammalian brain requires rapid changes in synaptic efficacy in response to glutamatergic activity, and engages similar cellular mechanisms to those that underlie long-term potentiation (LTP)[1]. If such changes in synaptic strength at a set of synapses cannot be stabilized, it is difficult to imagine how lasting memory traces could be formed[8]. The initial phase of early-LTP is supported by the post-translational modification or trafficking of existing proteins, whereas late-LTP lasting at least 4-6 h requires new protein synthesis[9].

In vitro studies indicate that that the events causing the upregulation of protein synthesis, in the soma or in dendrites, need not occur at exactly the same time as the trigger for LTP induction[10-21]. Two critical observations that underlie the 'synaptic tagging and capture' (STC) framework are: (1) Late-LTP in hippocampal area CA1 can be blocked by protein-synthesis inhibitors such as anisomycin, but prior strong tetanization of an independent input to an overlapping population of postsynaptic neurons stabilizes the decaying LTP[10]—in other words late-LTP can be induced without new protein synthesis at the time of induction if the relevant plasticity-related proteins have been synthesized beforehand. And (2) a strong tetanus can also 'rescue' decaying LTP induced by subsequent, or prior, weak tetanization of an independent input[10,11,13-19,21]. This extension of the time window for associative interactions during the stabilization of synaptic changes (sometimes called 'late associativity'), likely has important implications for our understanding of the association of information across time and the formation of lasting memories. According to the STC hypothesis, glutamatergic stimulation during memory encoding sets temporary 'tags' at activated synapses in a post-translational manner that then sequester plasticity-related proteins as they become available, thus stabilizing synaptic changes[22-24].

However, the phenomenon of STC has neither been reported nor validated *in vivo*. Much data has been gathered over the past 10 years concerning the molecular mechanisms underlying the STC process, extending to the level of individual dendritic spines[20], but it is not yet known whether the level of available proteins places significant restrictions on the persistence of synaptic changes *in vivo*. Spontaneous activity levels are reduced *in vitro*, neuromodulatory afferents are severed, and baseline levels of plasticity-related proteins are low if sufficient time is allowed for metabolic stabilization[25]. In the living animal, free from these artificial constraints on protein synthesis, the availability of relevant proteins may not limit the duration of synaptic changes; all synapses that are activated above a certain threshold—and tagged—might successfully capture the proteins necessary for lasting potentiation. In other words, the STC phenomenon might be specific to *in vitro* preparations, with no relevance in the intact animal.

Despite the need for an assessment of synaptic tagging and capture *in vivo*, the demand for two independent synaptic inputs to a common population of postsynaptic neurons presents a technical challenge[26]. In CA1 slices, two stimulating electrodes can be placed in the Schaffer collateral pathway, one on either side of a recording electrode in the stratum radiatum, but this configuration does not yield independent inputs in the intact animal. To overcome this difficulty, we chose to exploit the extensive long-range longitudinal connectivity of the Schaffer collateral / commissural system, in addition to the transverse connectivity that forms part of the 'traditional' trisynaptic circuit. The axons of CA3 are extensively collateralized, forming both associational connections with other CA3 cells, as well as the Schaffer collateral projection to CA1. Axons in both of these projections can extend for distances of several millimetres along the septotemporal (dorso-ventral) axis of

the hippocampus; the commissural projection comprises axons that cross the midline via the ventral hippocampal commissure and terminate in the contralateral hippocampus[27]. Functional and anatomical studies indicate that interhippocampal CA3-CA1 connectivity is maximal between regions located at equivalent septotemporal levels, and ipsilateral and contralateral projections converge on an overlapping population of CA1 neurons[28]. By placing stimulating electrodes bilaterally in CA3 at equivalent locations, independent populations of afferents to CA1 can be activated[29]. Using this arrangement, we set out to examine the phenomenon of synaptic tagging and capture in the living animal.

In experiment 1, we present evidence that strong tetanization can rescue decaying early-LTP induced by subsequent tetanization of a second input in the presence of the protein-synthesis inhibitor anisomycin ('strong-before-strong'[10]). In experiment 2, we show that early-LTP induced by weak tetanization can be stabilized by the later delivery of a strong tetanus to a second input ('weak before strong'[11]). In experiment 3, we investigate the dopamine-dependence of late-LTP induced by our strong-tetanus protocol. Overall, our results confirm that 'synaptic tagging and capture' can occur in the intact animal, and is not merely an artefact of *in vitro* hippocampal preparations.

Results

Independence of ipsilateral and contralateral projections

Bilateral stimulation of CA3 under urethane anaesthesia activated independent ipsilateral ($s1_i$) and contralateral ($s2_c$) populations of afferents converging on CA1 (Fig. 1). Owing to the challenging nature of the experimental set-up, and the need for long baseline periods to ensure signal stability, the time between the induction of anaesthesia and tetanization was typically 5-6 h, comparable to the incubation periods employed *in vitro* to minimize background levels of plasticity-related proteins[25].

'Strong-before-strong' protocol

Experiment 1 involved strong tetanization of pathway $s1_i$ after aCSF infusion ('strong + aCSF' group; n = 6), which induced persistent LTP lasting at least 5 h, relative to a non-tetanized contralateral control pathway ($s2_c$) (Fig. 2a & d). Intraventricular infusion of anisomycin before strong tetanization of $s1_i$ ('strong + ANI' group; n = 7) spared post-tetanic potentiation (PTP), and the early phase of LTP, but late-LTP was completely blocked; potentiation lasted approximately 3 h relative to the control pathway (Fig. 2b & d). Strong tetanization of $s2_c$ before anisomycin infusion and subsequent tetanization of $s1_i$ ('strong-before-strong + ANI' group) yielded late-LTP not only in $s2_c$, but also in $s1_i$, despite the fact that LTP in $s1_i$ was induces1d during the inhibition of protein synthesis (Fig. 2c & d). These results indicate that the persistence of LTP is dissociable from its initial strength, consistent with the STC hypothesis. An analysis of the opposite, mirror-image situation—the rescue of LTP in the contralateral projection ($s1_c$) by strong tetanization of the ipsilateral pathway ($s2_i$) in the same animals—is presented in Supplementary Figs. S1 & S2, and Table S1).

An ANOVA of the percentage fEPSP slope LTP 4-5 h after tetanization (Fig. 2d), with group ('strong + aCSF', 'strong + ANI', and 'strong-before-strong + ANI') as a between-subjects factor, and pathway ($s1_i$ and $s2_c$) as a within-subjects factor, revealed a group x pathway interaction [$F(2,19) = 4.81$; $p < 0.02$; Fig. 2d]. Following the overall ANOVA, a separate ANOVA of late-LTP in $s1_i$ only revealed a main effect of group [$F(2,19) = 3.86$; $p < 0.05$; Fig. 2d; left-hand panel]. *Post-hoc* comparisons (Fisher's LSD) revealed that anisomycin resulted in significantly lower late-LTP relative to that in aCSF-treated controls [$p < 0.02$], but prior tetanization of $s2_c$ resulted in a significant increase in late-LTP in $s1_i$

following anisomycin infusion [$p < 0.05$]; the resulting level of LTP did not differ from that in the aCSF-treated group [$p > 0.5$]; and was significantly above baseline [$t(8) = 3.94$; $p < 0.005$; one-sample t-test]. Analysis of simple main effects based on the overall ANOVA revealed significant differences between $s1_i$ and $s2_c$ in the 'strong + aCSF' group [$p < 0.005$], indicating significant late-LTP, but no difference was observed in the 'strong + ANI' group [$p > 0.6$]—LTP had decayed to baseline values in this case.

A main effect of group was also observed in $s2_c$ alone [$F(2,19) = 12.4$; $p < 0.001$; Fig. 2d; right-hand panel]. *Post-hoc* comparisons (Fisher's LSD) revealed that a strong tetanus to $s2_c$ in the 'strong-before-strong + ANI' group caused significant late-LTP relative to the aCSF control pathway [$p < 0.001$], and the anisomycin control pathway [$p < 0.0005$]; these control pathways did not differ from each other [$p > 0.6$].

At the dose used, anisomycin infusion typically caused a small but rapid increase in the fEPSP, followed by a gradual, but again slight, fall evident in the untetanized control pathway (Fig. 2b). However, control pathways did not differ significantly between aCSF- and anisomycin-treated groups 5 h after tetanization (see above), indicating that the block of late-LTP cannot be attributed to baseline effects. Group differences in post-tetanic potentiation (PTP; the mean slope during the 5-min period after the final tetanus train) and early-LTP (30-60 min after the final tetanus train) did not reach significance [$F < 1$ in both cases; ANOVA], indicating that anisomycin predominantly impaired late-LTP. Nonetheless, higher doses caused pronounced baseline changes (Fig. 3).

To assess the stability of rescued LTP, independently of its magnitude [18], we carried out an ANOVA of the percentage fEPSP slope LTP 30-60 min and 4-5 h after tetanization in the $s1_i$ pathways of the 'strong + ANI' (Fig. 2b), and 'strong-before-strong + ANI' (Fig. 2c) groups only. This analysis revealed a significant group x time interaction [$F(1,14) = 10.0$; $p < 0.001$], and a subsequent analysis of simple main effects revealed a significant decay of LTP between time points in the 'strong + ANI' group [$F(1,14) = 27.7$; $p < 0.001$], but no significant decline in the 'strong-before-strong + ANI' group [$F(1,14) = 1.41$; $p > 0.2$], confirming the stability of rescued late-LTP.

There were no group differences in stimulation intensity [$F < 1$; ANOVA] or fEPSP slope over the 1-h baseline period [$F(2,19) = 1.03$; $p > 0.3$]; fEPSP slopes in $s2_c$ were significantly smaller than in $s1_i$ [$F(1,19) = 17.9$; $p < 0.0005$], but stimulation intensity did not differ between pathways [$F < 1$]. Overall, no significant PPF was observed [$t(21) = 0.04$; $p > 0.9$; one-sample t-test; comparison to chance = 100%], and no group differences in values were obtained [$F < 1$]. See Table 1 for details.

'Weak-before-strong' protocol

Experiment 2 avoided the use of drugs. Strong tetanization of $s1_i$ ('strong-only' group; n = 7) induced robust late-LTP (Fig. 4a & d), whereas weak tetanization ('weak-only' group; n = 11) induced only a decaying early-LTP lasting approximately 3 h relative to the untetanized control pathway ($s2_c$) (Fig. 4b & d). However, strong tetanization of $s2_c$ after weak tetanization of $s1_i$ ('weak-before-strong' group; n = 11) not only induced late-LTP in $s2_c$, but also rescued late-LTP in $s1_i$ (Fig. 4c & d). In other words, decaying potentiation induced by weak tetanization can be converted into late-LTP by strong tetanization delivered later to an independent input. An analysis of the opposite, mirror-image situation —the rescue of LTP in the contralateral projection ($s1_c$) by strong tetanization of the ipsilateral pathway ($s2_i$)—is presented in Supplementary Figs. S1 & S3 and Table S1.

An ANOVA of the mean percentage fEPSP slope LTP 4-5 h after tetanization, with group ('weak only', 'strong only', and 'weak-before-strong') as a between-subjects factor, and

pathway ($s1_i$ and $s2_c$) as a within-subjects factor, revealed a group x pathway interaction [$F(2,26) = 9.35$; $p < 0.002$; Fig. 4d]. Following the overall ANOVA, a separate ANOVA of late-LTP in $s1_i$ only revealed a main effect of group [$F(2,26) = 11.9$; $p < 0.0005$; Fig. 4d; left-hand panel]. *Post-hoc* comparisons (Fisher's LSD) revealed that a weak tetanus to $s1_i$ caused significantly less late-LTP than a strong tetanus to $s1_i$ [$p < 0.0005$], but pathway $s1_i$ in the 'weak-before-strong' group showed significantly more late-LTP than the same pathway in the weak-only group [$p < 0.05$]—in other words a rescue of LTP was observed. Although the level of late-LTP in pathway $s1_i$ of the 'weak-before-strong' group remained below that observed in the strong-only group [$p < 0.001$], it was stable and the rescued LTP remained significantly above baseline 4-5 h after tetanization [$t(10) = 3.59$; $p < 0.005$; one-sample t-test]. Analysis of simple main effects based on the overall ANOVA revealed significant differences between pathways $s1_i$ and $s2_c$ in the strong-only group [$p < 0.002$], indicating significant late-LTP, but no difference was observed in the weakly tetanized group [$p > 0.6$]—LTP had decayed to baseline values in these animals. A separate analysis of LTP 5-6 h after tetanization gave similar results (Supplementary Fig. S4).

A main effect of group was also observed in $s2_c$ alone [$F(2,26) = 6.21$; $p < 0.01$; Fig. 4d, right-hand panel]. *Post-hoc* comparisons (Fisher's LSD) revealed that a strong tetanus to $s2_c$ in the 'weak-before-strong' group caused significant L-LTP relative to the strong-only control pathway [$p < 0.02$], and the weak-only control pathway [$p < 0.005$]; these control pathways did not differ from each other [$p > 0.6$].

Owing to the slightly smaller PTP induced by weak (versus strong) tetanization, there was a trend toward a significant overall group difference in PTP in $s1_i$ [$F(2,26) = 3.20$; $0.1 > p > 0.05$; ANOVA]. Similarly, an overall analysis of early-LTP (30-60 min after tetanization) revealed a significant group effect owing to the inclusion of the 'strong-only' group [$F(2,26) = 5.46$; $p < 0.02$]. Nevertheless, early-LTP did not differ between 'weak only' and 'weak-before-strong' groups [$p < 0.05$; Fisher's LSD], indicating that late-, but not early-LTP was significantly facilitated by the strong 'rescue' tetanus.

As in experiment 1, to assess the stability of rescued LTP induced by a weak tetanus, we conducted an ANOVA of the percentage fEPSP slope LTP 30-60 min and 4-5 h after tetanization in the $s1_i$ pathways of the 'weak only' (Fig. 4b), and 'weak-before-strong' (Fig. 4c) groups only. This analysis revealed a significant group x time interaction [$F(1,20) = 7.14$; $p < 0.02$], and a subsequent analysis of simple main effects revealed a significant decay of LTP between time points in the 'weak only' group [$F(1,20) = 30.4$; $p < 0.001$], but no significant decline in the 'weak-before-strong' group [$F(1,20) = 2.96$; $p > 0.1$].

There were no group differences in stimulation intensity or fEPSP slope over the 1-h baseline period [$F < 1$ in both cases; ANOVA]; fEPSP slopes in $s2_c$ were significantly smaller than in $s1_i$ [$F(1,26) = 44.7$; $p < 0.0005$], but stimulation intensity did not differ between pathways [$F < 1$]. Overall, no significant PPF was observed [$t(28) = 0.29$; $p > 0.7$; one-sample t-test; comparison to chance = 100%], and no group differences in values were obtained [$F < 1$]. See Table 1.

Owing to the slight baseline rise evident in Fig. 4c, data from 'weak-only' and 'weak-before-strong' groups were re-analysed after the exclusion of data from all animals in which baseline fEPSP slope values rose or fell by more than 10 percentage points between the first and last 20-min periods of the 1-h baseline in either $s1_i$ or $s2_c$ (an analysis that was possible owing to the relatively large n of 11 in these two groups originally). The re-analysed data are shown in Fig. 4e & f ('weak only': n = 8; 'weak-before-strong': n = 7). As expected, baseline values are stable, and the results are numerically very similar to those in Fig. 4b & c. An ANOVA of the mean percentage fEPSP slope LTP 4-5 h after tetanization—with

pathway as a within subjects factor and group as a between subjects factor—revealed a significant overall main effect of group [$F(1,13) = 12.8$; $p < 0.005$]. Comparison of late-LTP in pathway s1i of the 'weak-only' and 'weak-before-strong' groups revealed a significant difference [$F(1,13) = 6.52$; $p < 0.025$; analysis of simple main effects]; late-LTP in the latter group remained significantly above chance [$t(6) = 2.78$; $p < 0.05$; one-sample t-test]. As expected, the strong rescue tetanus resulted in significant potentiation relative to the untetanized control in the weak-only group [$F(1,13) = 7.92$; $p < 0.02$; analysis of simple main effects].

The role of dopamine

In experiment 3, we assessed the impact of the dopamine antagonist SCH23390 on late-LTP. Neither aCSF (Fig. 5a; n = 7) or SCH23390 (5 μg / μl; Fig. 5b; n = 7) blocked potentiation after 4 h (the point at which recording ended in this experiment), although a modest fall in both tetanized and control pathways was evident in the SCH23390 group by the end of the recording period. An ANOVA of LTP 3-4 h after tetanization revealed a difference between tetanized and non-tetanized pathways [$F(1,12) = 13.16$; $p < 0.005$], but no effect of drug group [$F(1,12) = 0.63$; $p > 0.4$], and no group x pathway interaction [$F(1,12) = 0.03$; $p > 0.8$]. Similarly, no group differences in PTP (0-5 min after tetanus) or early-LTP (30-60 min after tetanus) were observed in $s1_i$ [$F < 1$ in both cases]. Figure 5c shows the normalized fEPSP slope in each tetanized pathway expressed as a percentage of the value recorded in the corresponding control pathway, in order to control for baseline changes. When analysed in this way, the time course and level of potentiation was identical in SCH23390 and vehicle-treated groups.

No significant group [$F(1,12) = 0.08$; $p > 0.7$] or pathway [$F(1,12) = 2.07$; $p > 0.1$] differences were found in stimulation intensity; baseline fEPSP slope likewise did not differ between groups [$F(1,12 = 0.18$; $p > 0.6$], and on this occasion no differences were found between pathways $s1_i$ and $s2_c$ [$F(1,12) = 1.28$; $p > 0.2$]; see Table 1.

Discussion

The results of experiment 1 reveal that late-LTP of the ipsilateral Schaffer-collateral input to CA1 ($s1_i$) can be induced in the living rat during the inhibition of protein synthesis—a treatment that otherwise limits the duration of LTP to around 3 h—provided that strong tetanization of an independent contralateral commissural input ($s2_c$) occurs beforehand (Fig. 2). This suggests that proteins synthesized following strong tetanization of one pathway can subsequently be captured by tags set at the synapses of a separate input.

Doses of anisomycin comparable to that used here have previously been reported to block hippocampal LTP, long-term memory formation, and tetanus-induced protein synthesis[30-32]. A large number of proteins are up-regulated following the induction of late-LTP (e.g.[33]), and there is mounting evidence for the importance of local dendritic translation (e.g.[34-37]). Although we cannot rule out the possibility that anisomycin also blocks long-lasting changes in the intrinsic properties of neurons induced by strong tetanization[38], a cell-wide mechanism cannot explain the 'weak-before-strong' data of experiment 2 (see below), unless weak tetanization sets a synaptic tag as our hypothesis indicates that it must. In our hands, higher doses of anisomycin caused dose-dependent changes in baseline fEPSPs even in the absence of tetanization (Fig. 3), consistent with the multiple effects of anisomycin reported at doses higher than that used in the present study[32,39-41], including the suppression of neural activity[42]. However, no significant baseline changes were observed at the dose used in experiment 1.

Experiment 2 reveals that decaying early-LTP induced by weak tetanization of the ipsilateral CA3-CA1 projection ($s1_i$) can be converted into late-LTP by strong tetanization delivered later to the contralateral pathway ($s2_c$) (Fig. 4). The delivery of the strong 'rescue' tetanus *after* the weak tetanus excludes the possibility of sensitization, or a reduction in the threshold for the induction of late-LTP[11]; it is consistent with the setting of synaptic tags that subsequently capture proteins synthesized after the strong tetanus, and implies that the availability of plasticity-related proteins can indeed determine the duration of synaptic changes *in vivo*. Taken together, our results confirm the symmetrical nature of the synaptic tagging and capture process as characterized *in vitro*—strong tetanization can rescue decaying potentiation whether delivered before or after the latter's induction[10,11]. While we have focussed on the rescue of LTP in the uncrossed CA3-CA1 projection ($s1_i$) by strong tetanization of the crossed pathway ($s2_c$), the ability of strong ipsilateral CA3-CA1 tetanization to rescue decaying LTP in the contralateral projection was qualitatively similar, although statistically less robust (Supplementary Figs. S2 &S3), perhaps owing to the typically smaller and more variable levels of LTP seen in the crossed CA3-CA1 pathway[43].

In order to obtain independent synaptic inputs to a common pool of CA1 neurons, we stimulated bilaterally in CA3; our electrode locations yielded large fEPSPs in CA1 stratum radiatum following both ipsilateral and contralateral stimulation. The independence of crossed and uncrossed projections was confirmed by the absence of paired-pulse facilitation (PPF) following alternate stimulation of each pathway at an interval of 50 ms (Fig. 1d, middle bar); similarly, tetanization of one pathway caused no change in the other input. Although commissural projections to CA1 typically exhibit a denser pattern of termination in stratum oriens, relative to ipsilateral inputs that primarily target stratum radiatum, afferents originating from the intrahilar region are predominantly directed toward the contralateral stratum radiatum[44]. In view of this, the recording of large contralateral CA3-CA1 fEPSPs in stratum radiatum is consistent with our placement of stimulating electrodes toward the proximal (dentate) end of CA3. Although our experiments were conducted under urethane—an anaesthetic that suppresses fEPSPs, and necessitates the use of stronger tetanization protocols for LTP induction[45]—strong tetanization induced persistent LTP that was blocked by anisomycin (Fig. 2b), suggesting that protein-synthesis-dependent late-LTP can still be induced under these circumstances. Late-LTP typically lasted as long as stable recordings could be maintained (i.e. at least 5 h); in some instances, we observed stable LTP for over 10 h following strong tetanization.

Having established that synaptic tagging and capture can occur *in vivo*, it is necessary to identify physiologically plausible neural analogues of the strong tetanus—i.e. triggers for the heterosynaptic stabilization of synaptic potentiation induced by the activation of glutamate receptors. As the activation of dopaminergic afferents is a leading candidate for this role[46,47], the absence of an effect of dopamine receptor blockade on LTP induced by the strong tetanus used in the current series of experiments (Fig. 5) might seem surprising. The route of administration and dosage were chosen to match exactly those used in a previous behavioural study in which SCH23390 caused a marked impairment of long-term spatial-memory formation[48]. Moreover, dopamine D1/D5 receptor blockade can block CA1 late-LTP *in vivo*[49,50], and dopamine receptor activation can induce dendritic protein synthesis[51]. But despite the frequent focus on the dopaminergic innervation of CA1, there are likely to be multiple determinants of protein availability. For example, β-adrenergic activation facilitates a form of LTP requiring dendritic translation but not transcription[52], and somatic action potentials induced by alvear stimulation are sufficient to convert early to late-LTP in CA1[13]. In our experiments, it is likely that strong glutamatergic stimulation was sufficient to induce late-LTP without the additional requirement for dopaminergic activity; the activation of CaMKIV or metabotropic glutamate receptors might, for example, serve this function[18,53].

In fact, for anatomical reasons, the finding that our strong tetanus induces dopamine-independent LTP is fully consistent with the results obtained. The hippocampus receives dopaminergic inputs from mesolimbic structures such as the ventral tegmental area (VTA); afferents terminate in CA1, and to a lesser extent in CA3[54]. However, the axons of dopaminergic neurons exhibit limited collateralization, and only around 10 % of VTA dopaminergic neurons project contralaterally[54]. For these reasons, it is unlikely that tetanization of CA3 could result in a significant recruitment of dopaminergic fibres terminating contralaterally in CA1. In other words, the ability of a strong tetanus delivered to the crossed CA3-CA1 pathway to rescue decaying LTP in the ipsilateral projection is unlikely to be mediated by dopaminergic afferents. Nonetheless, dopamine is likely to play an important role in the stabilization of learning-induced synaptic changes triggered by physiological patterns of stimulation[48,55,56].

In summary, we find that the synaptic tagging and capture phenomenon, consistent with its hypothesized role in memory[57,58,55] , is not limited to *in vitro* preparations. As well as providing a mechanism for the association of information over time, our use of long-range commissural projections to provide the 'rescue' stimulus indicates that the information to be associated can originate from cells located in opposite hemispheres of the brain. In other words, the 'late associativity' of LTP operates not only over an extended time-frame, but also over a distance of several millimetres in the living rat. Our findings provide a bridge between investigations of behavioural tagging in freely moving animals and *in vitro* studies of underlying mechanisms, and so validate further work aimed at uncovering the molecular basis of memory persistence.

Methods

Subjects

All procedures were conducted in accordance with the UK Animals (Scientific Procedures) Act (1986). Prior to the experiment, adult male Lister-hooded rats (250-500 g; n = 91) were given *ad libitum* access to food and water and maintained on a 12 h light / 12 h dark cycle.

Anaesthesia

Rats were anaesthetized with urethane (ethyl carbamate; 1.5 g / kg; 0.3 mg / ml, i.p.), injected with carprofen (Rimadyl small animal solution, 4 mg / kg; s.c.), and placed in a stereotaxic frame with the skull horizontal. Body temperature was monitored by a rectal probe and maintained at 36.2 °C using an isothermic heating blanket. Depth of anaesthesia was assessed throughout the experiment, and urethane top-ups of 0.2 ml were administered as required. Breathing rate was monitored continuously using a light-dependent resistor to detect thoracic movements, and analysed online using in-house software. If breathing fell below 70 breaths / min, rats received an injection of atropine (0.4 mg / kg; s.c.) or doxapram (5 mg / kg; i.p.). Subcutaneous injections of a glucose / saline mixture were administered every 3 h to maintain hydration (1.5 ml of 0.9 % saline + 0.5 ml of 5 % glucose).

Electrophysiological recording

PTFE-insulated monopolar platinum / iridium recording electrodes (diameter = 0.103 mm) were lowered bilaterally into the stratum radiatum of area CA1 (3.8 mm posterior and 2.5 mm lateral to bregma; depth approximately −2.5 mm from dura). Bipolar stimulating electrodes comprising 2 twisted wires identical in composition to the recording electrodes were lowered bilaterally into CA3 (3.5 mm posterior and 3.0 mm lateral to bregma; depth approximately −3.0 mm from dura) in order to activate independent populations of synaptic contacts made by ipsilateral Schaffer collateral ($s1_i$) and contralateral commissural projections ($s2_c$) converging on the same neuronal populations sampled by each of the

recording electrodes. Fig. 1a shows a photomicrograph of representative marking lesions made at both stimulating sites and the left-hand recording site in an individual rat. A schematic illustration of the electrode locations and pathways stimulated is shown Fig. 1b; for simplicity, CA3-CA3 projections are omitted, and only a single pair of ipsilateral and contralateral projections is shown; in practice CA3 stimulation simultaneously activates crossed and uncrossed afferents, and recording electrodes were placed bilaterally to capitalize on this (Supplementary Fig. S1). Nonetheless; in our main analysis (Figs. 2 & 4), we focus solely on the rescue of LTP in an ipsilateral CA3-CA1 projection ($s1_i$) by strong tetanization of the crossed CA3-CA1 pathway ($s2_c$) converging on the same recording site. Note that the hemisphere (left or right) containing the ipsilateral projection of interest ($s1_i$) was varied over days in a quasi-random fashion. An analysis of the opposite, mirror-image situation—the rescue of LTP in the contralateral projection ($s1_c$) by strong tetanization of the ipsilateral pathway ($s2_i$) in the same animals—is presented in the Supplementary Information (Supplementary Figs. S2 & S3).

Throughout the experiment, fEPSPs were amplified and sampled at 20 kHz using a PC running custom-written LabView software developed by Patrick Spooner; fEPSP amplitude and initial slope (measured by linear regression between two fixed time points) were monitored on-line. Stimulation was delivered under computer control via a Neurolog system (NL800A; Digitimer LTD, Herts., UK), and consisted of biphasic constant-current pulses. At the start of each experiment, electrodes were lowered into the hippocampus, and depths were adjusted to maximize the amplitude of the negative-going dendritic fEPSPs elicited in CA1 by stimulation of CA3; typical depth profiles are shown in Fig. 6 (see Supplementary Methods for further information). Stimulation intensity was adjusted to elicit a contralateral fEPSP of approximately 3 mV in amplitude (200-500 μA). Representative fEPSPs evoked by stimulation of $s1_i$ and $s2_c$ are shown in Fig. 1C & Fig. 6. Table 1 shows mean stimulation intensities and baseline fEPSP slopes for all experiments, groups, and pathways.

The independence of $s1_i$ and $s2_c$ was confirmed at the start of the experiment in each animal by the delivery of pairs of biphasic stimulation pulses (50 μs per phase) to $s2_c$ followed by $s1_i$ at an interval of 50 ms (6 pairs; 10-s intra-pair interval), followed by single test pulses delivered to $s1_i$ only (6 pulses). PPF was calculated by expressing the mean fEPSP slope recorded in $s1_i$ after stimulation of $s2_c$ as a percentage of the value obtained in $s1_i$ without prior stimulation. Mean data from all experiments reported in Figs. 2 & 4 are shown in Fig. 1d (middle panel) and Table 1. Paired stimulation was delivered first to $s2_c$, then to $s1_i$, as stimulation in the opposite sequence typically causes a modest paired-pulse depression of $s2_c$, a phenomenon that has been reported previously, and attributed to the recruitment of feed-forward and feedback inhibition by ipsilateral stimulation[59].

After electrode placement, and a check for the absence of PPF, baseline recording began; single biphasic test pulses (50 μs pulse width per phase) were delivered alternately to each stimulating electrode at 2-min intervals. The decision regarding the experiment to be conducted on any given day was always made prior to the start of baseline recording, with experiments alternating between groups across days. After a baseline period typically lasting several hours, and once stable fEPSPs had been observed for at least 1 h, tetanic stimulation began. Pulse width (per phase) was increased to 100 μs during a high-frequency tetanus. Strong tetanization consisted of 3 trains of 50 pulses at 250 Hz, with a 5-min inter-train interval; a weak tetanus comprised 1 train of 50 pulses at 100 Hz. Data obtained from a specific recording electrode were discounted if the fEPSP slope elicited by ipsilateral or bilateral stimulation fell to 60 % of the baseline value or below within 4-5 h of tetanization (or the corresponding time point for untetanized pathways). In all cases, fEPSP slope data were normalized to the mean of the 1-h baseline period (assigned a value of 100%), and group means were calculated.

Drugs

An anisomycin solution was prepared by dissolving the powdered drug (Sigma-Aldrich, UK) in equimolar HCl and diluting with artificial cerebrospinal fluid (aCSF; in millimolar: 150 Na+, 3 K+, 1.4 Ca2+, 0.8 Mg 2+, 155 Cl−, 0.2 H2PO4−, 0.8 HPO42−, in pyrogen-free water at pH 7.2). The pH of the anisomycin solution was adjusted to 7.2 by the addition of NaOH, and the final concentration was 5 mg / ml. Powdered SCH23390 (Sigma-Aldritch, UK) was dissolved in sterile aCSF to yield a concentration of 5 mg/ml. Solutions were vortexed, gently sonicated, and stored in small aliquots at −20 C prior to use.

Drug administration and time lines

In experiment 1, bilateral intraventricular (i.c.v.) infusion cannulae (24 gauge stainless steel) were lowered into the left and right lateral ventricles at the same time as electrode placement (co-ordinates: 0.9 mm posterior and 1.3 mm lateral to bregma; depth = −4.5 mm from the skull surface). Bilateral i.c.v. infusions (5 μl per ventricle over 10 min) were delivered via 5 μl SGE syringes mounted in a syringe pump (World Precision Instruments, Stevenage, UK), and connected to the infusion cannulae with plastic tubing. Control groups received a bilateral i.c.v. infusion (5 μl per ventricle over 10 min) of either anisomycin (5 μg/μl) or aCSF starting 15 min before strong tetanization of $s1_i$. In the 'rescue' group, a strong tetanus was delivered to $s2_c$ ending 15 min before infusion of anisomycin and subsequent strong tetanization of s1i; recording continued for a further 5 h. In experiment 2 (Fig. 4), control groups received either strong or weak tetanization of $s1_i$ in the absence of infusion; in the 'rescue' group, $s1_i$ received weak tetanization 30 min before strong tetanization of $s2_c$; recording continued for a further 5 h.

In experiment 3, intra-hippocampal infusion cannulae were implanted under recoverable anaesthesia prior to electrophysiological recording. Rats were anaesthetized with isoflurane, injected with Rimadyl (carfrofen; 5 mg / kg, s.c.), and placed in a stereotaxic frame with the skull horizontal. Guide cannulae (outer diameter = 0.46 mm; Plastics One) were implanted bilaterally into the dorsal hippocampus (co-ordinates from bregma: AP = −4.5 mm; Lat. = 3.0 mm; DV from dura = 2.5 mm). These were fixed in place using dental cement, and the headcap was secured to the skull using jewellers' screws. To prevent blockage or infection, dummy cannulae (or stylets; outer diameter = 0.2 mm, protruding 0.5 mm from the end of the guide cannulae) were inserted into the guides during the recovery period. After approximately 1 week, the rats were anaesthetized with urethane for electrophysiological recording. After stable baseline recordings were obtained, injection needles were inserted into the guide cannulae. These were connected via plastic tubing to SGE syringes mounted in a syringe driver, and protruded 0.5 mm from the ends of the guide cannulae (i.e. the infusion site was −3.0 mm from the dura). Intrahippocampal infusions of either aCSF or SCH23390 (5 μg / μl; 1μl per hippocampus) were delivered over 5 min, starting 15 min before strong tetanization of $s1_i$. Post-tetanus recording continued for 4 h in Experiment 3, rather than 5 h in Experiments 1 & 2. In order to control for infusion-induced baseline changes, after normalization with respect to baseline values (see above), fEPSP slopes in $s1_i$ (tetanized pathway) were subsequently expressed as a percentage of the corresponding values in $s2_c$ (control pathway) for each animal and time point.

Histology

At the end of experiments 1-3, marking lesions were made by the delivery of biphasic 1 mA constant-current pulses (1 s / phase) to both stimulating and recording electrodes. Rats were killed by cervical dislocation and brains were removed and stored in 10 % formalin. 30 μm coronal sections through the hippocampus were then cut using a cryostat: 1 in 3 sections was mounted on a slide and stained with cresyl violet. After examination under a light microscope, stimulation sites were marked on the appropriate coronal section taken from the

Paxinos and Watson (2005) atlas[60]. All electrodes were correctly positioned (Figs. 7 & Supplementary Fig. S5), and, in experiment 1, all infusion cannulae were located in the lateral ventricles.

Supplementary Material

Refer to Web version on PubMed Central for supplementary material.

Acknowledgments

This work was supported by a Wellcome Trust Project Grant held by S.J.M. (WT083601MA). We thank Patrick Spooner for programming, electronics, and computing support, Jane Tulloch for assistance with histology, and the members of the CCNS for discussion and advice.

References

1. Martin SJ, Grimwood PD, Morris RGM. Synaptic plasticity and memory: an evaluation of the hypothesis. Annu. Rev. Neurosci. 2000; 23:649–711. [PubMed: 10845078]
2. Wiesel TN, Hubel DH. Single-cell responses in striate cortex of kittens deprived of vision in one eye. J. Neurophysiol. 1963; 26:1003–1017. [PubMed: 14084161]
3. Bienenstock EL, Cooper LN, Munro PW. Theory for the development of neuron selectivity: orientation specificity and binocular interaction in visual cortex. J. Neurosci. 1982; 2:32–48. [PubMed: 7054394]
4. Hubener M, Bonhoeffer T. Searching for engrams. Neuron. 2010; 67:363–371. [PubMed: 20696375]
5. Hawkins RD, Kandel ER, Bailey CH. Molecular mechanisms of memory storage in Aplysia. Biol. Bull. 2006; 210:174–191. [PubMed: 16801493]
6. Turrigiano GG. The self-tuning neuron: synaptic scaling of excitatory synapses. Cell. 2008; 135:422–435. [PubMed: 18984155]
7. Gross CG. Neurogenesis in the adult brain: death of a dogma. Nature Rev. Neurosci. 2000; 1:67–73. [PubMed: 11252770]
8. Dudai, Y.; Morris, RGM. To consolidate or not to consolidate: What are the questions?. In: Bolhuis, JJ., editor. Brain, Perception, Memory. Advances in Cognitive Sciences. Oxford University Press; Oxford, UK: 2000.
9. Abraham WC, Williams JM. LTP maintenance and its protein synthesis-dependence. Neurobiol. Learn. Mem. 2008; 89:260–268. [PubMed: 17997332]
10. Frey U, Morris RGM. Synaptic tagging and long-term potentiation. Nature. 1997; 385:533–536. [PubMed: 9020359]
11. Frey U, Morris RGM. Weak before strong: dissociating synaptic tagging and plasticity-factor accounts of late-LTP. Neuropharmacology. 1998; 37:545–552. [PubMed: 9704995]
12. Martin KC, et al. Synapse-specific, long-term facilitation of aplysia sensory to motor synapses: a function for local protein synthesis in memory storage. Cell. 1997; 91:927–938. [PubMed: 9428516]
13. Dudek SM, Fields RD. Somatic action potentials are sufficient for late-phase LTP-related cell signaling. Proc. Natl. Acad. Sci. USA. 2002; 99:3962–3967. [PubMed: 11891337]
14. O'Carroll CM, Morris RGM. Heterosynaptic co-activation of glutamatergic and dopaminergic afferents is required to induce persistent long-term potentiation. Neuropharmacology. 2004; 47:324–332. [PubMed: 15275821]
15. Young JZ, Nguyen PV. Homosynaptic and heterosynaptic inhibition of synaptic tagging and capture of long-term potentiation by previous synaptic activity. J. Neurosci. 2005; 25:7221–7231. [PubMed: 16079404]
16. Alarcon JM, Barco A, Kandel ER. Capture of the late phase of long-term potentiation within and across the apical and basilar dendritic compartments of CA1 pyramidal neurons: synaptic tagging is compartment restricted. J. Neurosci. 2006; 26:256–264. [PubMed: 16399695]

17. Sajikumar S, Li Q, Abraham WC, Xiao ZC. Priming of short-term potentiation and synaptic tagging/capture mechanisms by ryanodine receptor activation in rat hippocampal CA1. Learn. Mem. 2009; 16:178–186. [PubMed: 19223601]
18. Redondo RL, et al. Synaptic tagging and capture: differential role of distinct calcium/calmodulin kinases in protein synthesis-dependent long-term potentiation. J. Neurosci. 2010; 30:4981–4989. [PubMed: 20371818]
19. Lu Y, et al. TrkB as a potential synaptic and behavioral tag. J. Neurosci. 2011; 31:11762–11771. [PubMed: 21849537]
20. Govindarajan A, Israely I, Huang SY, Tonegawa S. The dendritic branch is the preferred integrative unit for protein synthesis-dependent LTP. Neuron. 2011; 69:132–146. [PubMed: 21220104]
21. Fonseca R. Activity-dependent actin dynamics are required for the maintenance of long-term plasticity and for synaptic capture. Eur. J. Neurosci. 2012; 35:195–206. [PubMed: 22250814]
22. Frey U, Morris RGM. Synaptic tagging: implications for late maintenance of hippocampal long-term potentiation. Trends Neurosci. 1998; 21:181–188. [PubMed: 9610879]
23. Martin KC, Kosik KS. Synaptic tagging -- who's it? Nat. Rev. Neurosci. 2002; 3:813–820. [PubMed: 12360325]
24. Redondo RL, Morris RGM. Making memories last: the synaptic tagging and capture hypothesis. Nat. Rev. Neurosci. 2011; 12:17–30. [PubMed: 21170072]
25. Sajikumar S, Navakkode S, Frey JU. Protein synthesis-dependent long-term functional plasticity: methods and techniques. Curr. Opin. Neurobiol. 2005; 15:607–613. [PubMed: 16150586]
26. Hassan H, Frey S, Frey JU. Search for a two-input model for future investigations of 'synaptic tagging' in freely moving animals in vivo. J. Neurosci. Methods. 2006; 152:220–228. [PubMed: 16216335]
27. Amaral DG, Witter MP. The three-dimensional organization of the hippocampal formation: a review of anatomical data. Neuroscience. 1989; 31:571–591. [PubMed: 2687721]
28. Buzsaki G, Eidelberg E. Convergence of associational and commissural pathways on CA1 pyramidal cells of the rat hippocampus. Brain Res. 1982; 237:283–295. [PubMed: 7082996]
29. Staubli U, Scafidi J. Time-dependent reversal of long-term potentiation in area CA1 of the freely moving rat induced by theta pulse stimulation. J. Neurosci. 1999; 19:8712–8719. [PubMed: 10493772]
30. Mullany P, Lynch MA. Changes in protein synthesis and synthesis of the synaptic vesicle protein, synaptophysin, in entorhinal cortex following induction of long-term potentiation in dentate gyrus: an age-related study in the rat. Neuropharmacology. 1997; 36:973–980. [PubMed: 9257941]
31. Meiri N, Rosenblum K. Lateral ventricle injection of the protein synthesis inhibitor anisomycin impairs long-term memory in a spatial memory task. Brain Res. 1998; 789:48–55. [PubMed: 9602054]
32. Wanisch K, Wotjak CT. Time course and efficiency of protein synthesis inhibition following intracerebral and systemic anisomycin treatment. Neurobiol. Learn. Mem. 2008; 90:485–494. [PubMed: 18395476]
33. McNair K, Davies CH, Cobb SR. Plasticity-related regulation of the hippocampal proteome. Eur. J. Neurosci. 2006; 23:575–580. [PubMed: 16420465]
34. Sutton MA, Schuman EM. Local translational control in dendrites and its role in long-term synaptic plasticity. J. Neurobiol. 2005; 64:116–131. [PubMed: 15883999]
35. Richter JD, Klann E. Making synaptic plasticity and memory last: mechanisms of translational regulation. Genes Dev. 2009; 23:1–11. [PubMed: 19136621]
36. Bramham CR, et al. The Arc of synaptic memory. Exp. Brain Res. 2010; 200:125–140. [PubMed: 19690847]
37. Doyle M, Kiebler MA. Mechanisms of dendritic mRNA transport and its role in synaptic tagging. EMBO J. 2011; 30:3540–3552. [PubMed: 21878995]
38. Cohen-Matsliah SI, Motanis H, Rosenblum K, Barkai E. A novel role for protein synthesis in long-term neuronal plasticity: maintaining reduced postburst afterhyperpolarization. J. Neurosci. 2010; 30:4338–4342. [PubMed: 20335469]

39. Rudy JW. Is there a baby in the bathwater? Maybe: some methodological issues for the de novo protein synthesis hypothesis. Neurobiol. Learn. Mem. 2008; 89:219–224. [PubMed: 17928242]
40. Alberini CM. The role of protein synthesis during the labile phases of memory: revisiting the skepticism. Neurobiol. Learn. Mem. 2008; 89:234–246. [PubMed: 17928243]
41. Qi Z, Gold PE. Intrahippocampal infusions of anisomycin produce amnesia: contribution of increased release of norepinephrine, dopamine, and acetylcholine. Learn. Mem. 2009; 16:308–314. [PubMed: 19403793]
42. Sharma AV, Nargang FE, Dickson CT. Neurosilence: profound suppression of neural activity following intracerebral administration of the protein synthesis inhibitor anisomycin. J. Neurosci. 2012; 32:2377–2387. [PubMed: 22396412]
43. Kaibara T, Leung LS. Basal versus apical dendritic long-term potentiation of commissural afferents to hippocampal CA1: a current-source density study. J. Neurosci. 1993; 13:2391–2404. [PubMed: 8501513]
44. Laurberg S. Commissural and intrinsic connections of the rat hippocampus. J. Comp. Neurol. 1979; 184:685–708. [PubMed: 422759]
45. Riedel G, Seidenbecher T, Reymann KG. LTP in hippocampal CA1 of urethane-narcotized rats requires stronger tetanization parameters. Physiol. Behav. 1994; 55:1141–1146. [PubMed: 8047583]
46. Frey S, Frey JU. 'Synaptic tagging' and 'cross-tagging' and related associative reinforcement processes of functional plasticity as the cellular basis for memory formation. Prog. Brain Res. 2008; 169:117–143. [PubMed: 18394471]
47. Lisman JE, Grace AA. The hippocampal-VTA loop: controlling the entry of information into long-term memory. Neuron. 2005; 46:703–713. [PubMed: 15924857]
48. O'Carroll CM, Martin SJ, Sandin J, Frenguelli B, Morris RGM. Dopaminergic modulation of the persistence of one-trial hippocampus-dependent memory. Learn. Mem. 2006; 13:760–769. [PubMed: 17142305]
49. Swanson-Park JL, et al. A double dissociation within the hippocampus of dopamine D1/D5 receptor and beta-adrenergic receptor contributions to the persistence of long-term potentiation. Neuroscience. 1999; 92:485–497. [PubMed: 10408599]
50. Lemon N, Manahan-Vaughan D. Dopamine D1/D5 receptors gate the acquisition of novel information through hippocampal long-term potentiation and long-term depression. J. Neurosci. 2006; 26:7723–7729. [PubMed: 16855100]
51. Smith WB, Starck SR, Roberts RW, Schuman EM. Dopaminergic stimulation of local protein synthesis enhances surface expression of GluR1 and synaptic transmission in hippocampal neurons. Neuron. 2005; 45:765–779. [PubMed: 15748851]
52. O'Dell TJ, Connor SA, Gelinas JN, Nguyen PV. Viagra for your synapses: Enhancement of hippocampal long-term potentiation by activation of beta-adrenergic receptors. Cell. Signal. 2010; 22:728–736. [PubMed: 20043991]
53. Anwyl R. Metabotropic glutamate receptor-dependent long-term potentiation. Neuropharmacology. 2007; 56:735–740. [PubMed: 19705571]
54. Gasbarri A, Sulli A, Packard MG. The dopaminergic mesencephalic projections to the hippocampal formation in the rat. Prog. Neuropsychopharmacol. Biol. Psychiatry. 1997; 21:1–22. [PubMed: 9075256]
55. Wang SH, Redondo RL, Morris RGM. Relevance of synaptic tagging and capture to the persistence of long-term potentiation and everyday spatial memory. Proc. Natl. Acad. Sci. USA. 2010; 107:19537–19542. [PubMed: 20962282]
56. Bethus I, Tse D, Morris RGM. Dopamine and memory: modulation of the persistence of memory for novel hippocampal NMDA receptor-dependent paired associates. J. Neurosci. 2010; 30:1610–1618. [PubMed: 20130171]
57. Moncada D, Viola H. Induction of long-term memory by exposure to novelty requires protein synthesis: evidence for a behavioral tagging. J. Neurosci. 2007; 27:7476–7481. [PubMed: 17626208]

58. Ballarini F, Moncada D, Martinez MC, Alen N, Viola H. Behavioral tagging is a general mechanism of long-term memory formation. Proc. Natl. Acad. Sci. USA. 2009; 106:14599–604. [PubMed: 19706547]

59. Leung LS, Peloquin P, Canning KJ. Paired-pulse depression of excitatory postsynaptic current sinks in hippocampal CA1 in vivo. Hippocampus. 2008; 18:1008–1020. [PubMed: 18548580]

60. Paxinos, G.; Watson, C. The Rat Brain in Stereotaxic Coordinates. Elsevier Academic; Amsterdam: 2005.

Europe PMC Funders Author Manuscripts

Europe PMC Funders Author Manuscripts

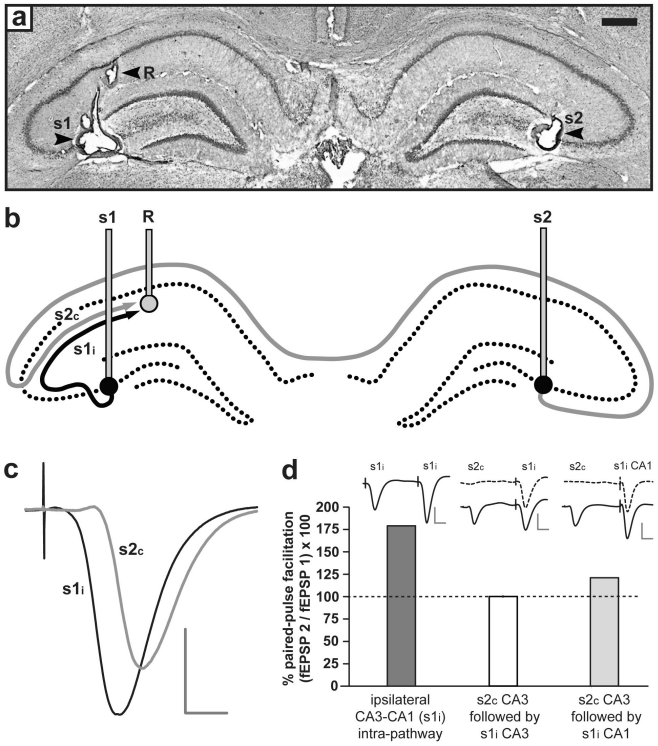

Figure 1. Experimental set-up

(**a**) Photomicrograh of coronal sections indicating the location of bilateral stimulating electrodes in CA3 (s1 and s2) and a recording electrode in left CA1 (R); the right-hand recording electrode was visible only in a slightly more posterior section. Arrows indicate the location of marking lesions made at the electrode tips; scale bar = 0.5 mm. (**b**) Schematic diagram of stimulating and recording sites (s1 and s2), and ipsilateral and contralateral CA3-CA1 projections ($s1_i$ and $s2_c$). In this example, both pathways converge on a common population of neurons whose synaptic responses are sampled by the left-hand recording electrode, R. For simplicity, CA3-CA3 projections are omitted (see Supplementary Methods) (**c**) Representative fEPSPs evoked by stimulation of $s1_i$ and $s2_c$. Note the longer latency and smaller amplitude of the contralateral fEPSP (scale bar: vertical = 2 mV; horizontal = 5 ms). (**d**) Intra-pathway paired stimulation at an interval of 50 ms yielded pronounced paired-pulse facilitation (PPF) of the fEPSP slope; the left-hand bar shows a single example of PPF in the ipsilateral CA3-CA1 projection; examples of fEPSPs elicited by paired stimulation are shown. However, PPF was absent after stimulation of $s2_c$ followed by $s1_i$ at an interval of 50 ms; the middle bar shows mean (± SEM) PPF for all experiments reported in Figs. 2 & 4 (n = 51), a value that did not differ from chance (100 %) [100.2 ± 0.8; t(50) = 0.20; p > 0.8; one-sample t-test], confirming the independence of the 2 pathways. Independence was compromised if one or both stimulating electrodes were raised into CA1; the right-hand bar shows an example of modest PPF obtained in a single rat by paired stimulation of contralateral CA3 followed by ipsilateral CA1, indicating that the two stimulators now activate partially overlapping populations of afferents. Examples of fEPSPs elicited by stimulation of $s1_i$ with (solid line) or without (dashed line) prior stimulation of $s2_c$ are shown above the middle and right-hand bars (scale bar: vertical = 4 mV; horizontal = 10 ms).

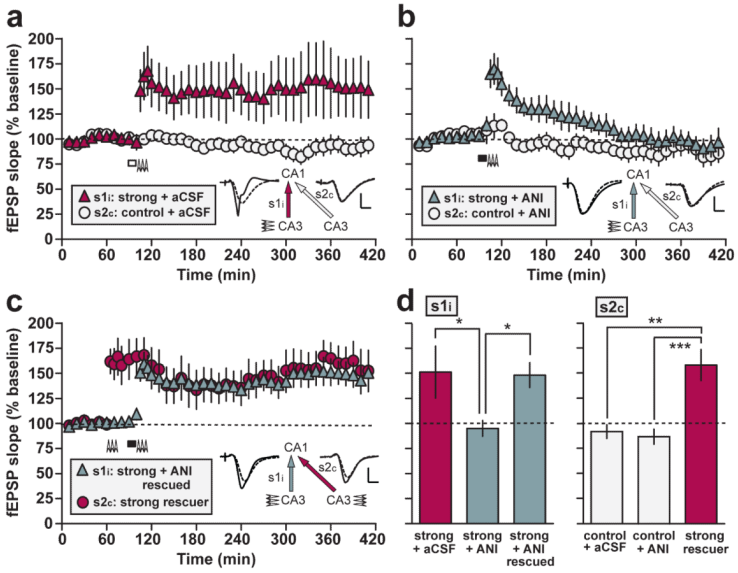

Figure 2. Strong-before-strong protocol

(**a**) Bilateral intraventricular infusion of aCSF (white rectangle) starting 15 min before strong tetanization of $s1_i$ (arrowheads) had no effect on late-LTP in $s1_i$ ('strong + aCSF'; n = 6). (**b**) Infusion of anisomycin (black rectangle) completely blocked late LTP in $s1_i$ ('strong + ANI'; n = 7). (**c**) The addition of a strong tetanus to $s2_c$ ending 15 min before the start of anisomycin infusion and tetanization of $s1_i$ resulted in late-LTP in both pathways ('strong-before-strong + ANI' group, comprising 'strong + ANI rescued' and 'strong rescuer' pathways; n = 9). Sample fEPSPs recorded in $s1_i$ and $s2_c$ before (dotted line) and 5 h after tetanization (solid line) are shown (scale bars for a-c: vertical = 2 mV; horizontal = 5 ms). (**d**) Mean fEPSP slope values recorded for $s1_i$ and $s2_c$ in all experimental groups between 4-5 h after the relevant tetanus, and normalized to the mean of the 1-h baseline period. Asterisks indicate significant group differences in late-LTP (*p < 0.05; **p < 0.01; ***p < 0.001; *post-hoc* comparisons—Fisher's LSD). All data are plotted as mean ± SEM.

Europe PMC Funders Author Manuscripts

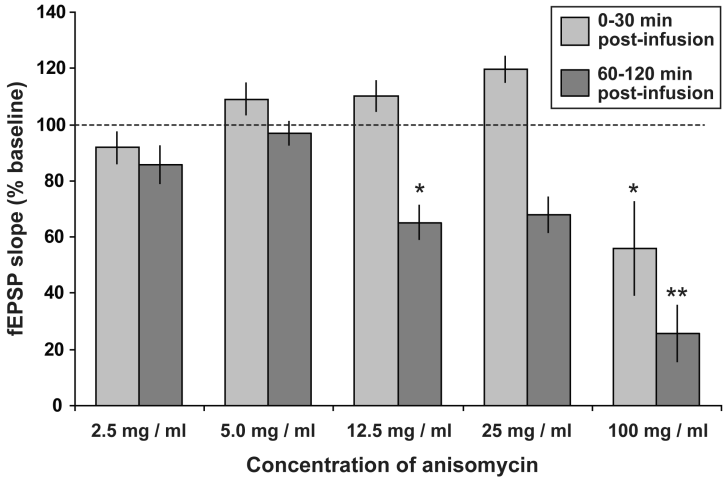

Figure 3. Dose-dependent depression of the fEPSP slope by higher doses of anisomycin

fEPSP slope 0-30 min and 60-120 min after the end of drug infusion (as a percentage of the value recorded during a 30-min baseline period) is plotted for a range of doses of anisomycin (expressed as μg / μl). All doses were delivered in a total volume of 10 μl (5 μl per ventricle) over 10 min. As the effects of anisomycin were proportionally similar in both ipsilateral and contralateral CA3-CA1 pathways, data from all pathways were combined in this analysis [2.5 μg / μl: n = 6 (3 rats); 5.0 μg / μl: n = 13 (8 rats; data from all control pathways in 'ANI + strong' group, Fig. 2); 12.5 μg / μl: n = 4 (1 rat); 25 μg / μl: n = 4 (1 rat); 100 μg / μl: n = 8 (2 rats)]. A main effect of dose was observed both 0-30 min [$F(4,30) = 6.15$; $p < 0.002$] and 60-120 min post-infusion [$F(4,30) = 19.3$; $p < 0.001$]. Asterisks indicate significant deviations from baseline (100 %; ** $p < 0.01$; * $p < 0.05$; one-sample t-tests with Bonferroni correction). All data are plotted as mean ± SEM.

Europe PMC Funders Author Manuscripts

Europe PMC Funders Author Manuscripts

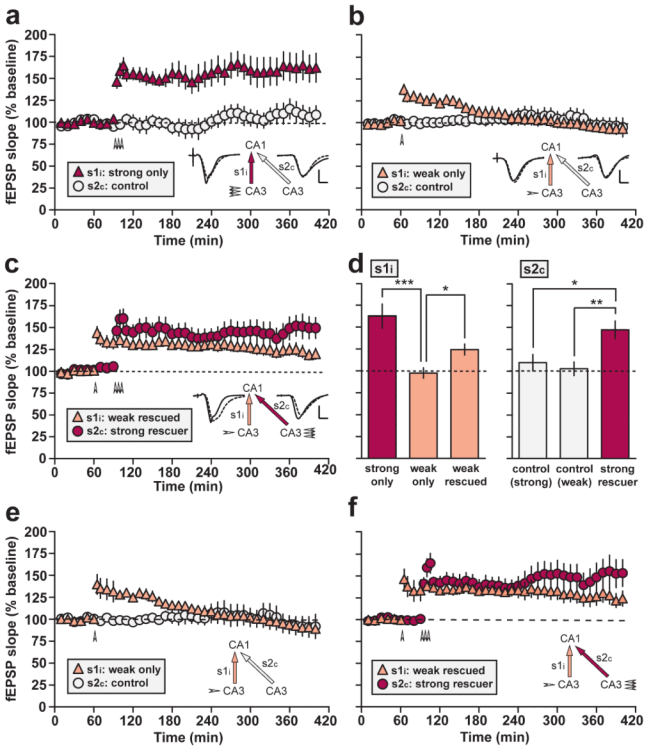

Figure 4. Weak-before-strong protocol

(**a**) Strong tetanization (arrowheads) of ipsilateral CA3 ($s1_i$) induced stable late-LTP ('strong only'; n = 7). (**b**) Weak tetanization of $s1_i$ (arrowhead) induced decremental early-LTP that reached baseline within approximately 3 h ('weak only'; n =11). (**c**) Strong tetanization of $s2_c$ 30 min after weak tetanization of $s1_i$ resulted in late-LTP in both pathways ('weak-before-strong'; n = 11). Sample fEPSPs recorded in $s1_i$ and $s2_c$ before (dotted line) and 5 h after tetanization (solid line) are shown in **a-c** (scale bar: vertical = 2mV; horizontal = 5ms). (**d**) Mean normalized fEPSP slope in $s1_i$ and $s2_c$ recorded 4-5 h after tetanization in all groups. Asterisks indicate significant differences in late-LTP between groups (*p < 0.05; **p < 0.01; ***p < 0.001; *post-hoc* comparisons—Fisher's LSD). (**e & f**) Re-analysis of 'weak-only' (**e**; n = 8) and 'weak-before-strong' (**f**; n = 7) data after the exclusion of data from all animals in which baseline fEPSP slope values fell by more than 10 percentage points between the first and last 20-min periods of the 1-h baseline in either $s1_i$ or $s2_c$. The pattern of results is identical to that observed in b and c. All data are plotted as mean ± SEM.

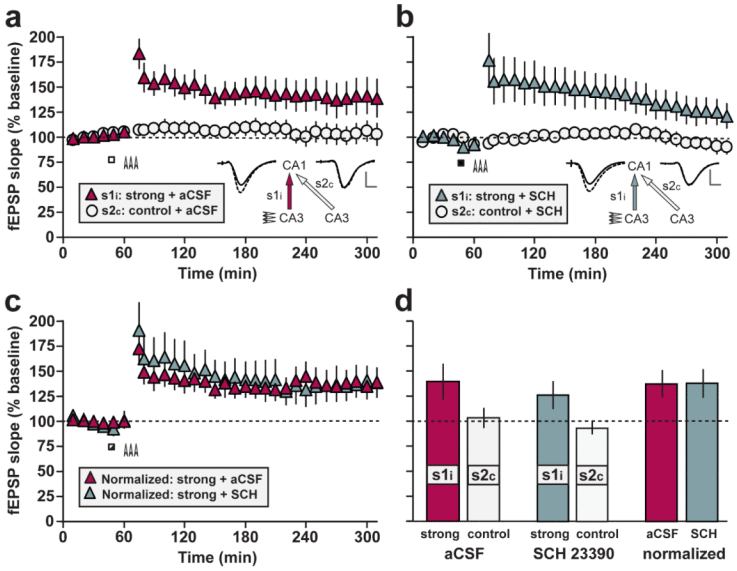

Figure 5. Dopamine and late LTP

(**a**) Bilateral intraventricular infusion of aCSF (n = 7; white rectangle) starting 15 min before strong tetanization of $s1_i$ (arrowheads) had no effect on late-LTP in $s1_i$. (**b**) Despite a slight baseline fall in both $s1_i$ and $s2_c$ after infusion, SCH23390 (n = 7; black rectangle) likewise failed to block late-LTP. Sample fEPSPs recorded in $s1_i$ and $s2_c$ before (dotted line) and 4 h after tetanization (solid line) are shown in **a** & **b** (scale bar: vertical = 2mV; horizontal = 5ms). (**c**) In order to eliminate the possible influence of infusion-related baseline changes, values in $s1_i$ were normalized, in each animal, to those in $s2_c$ and the mean data were re-plotted (see Methods). SCH23390 had no effect on normalized levels of LTP. The point of drug infusion is indicated by a black-and-white rectangle. All data are plotted as mean ± SEM.

Europe PMC Funders Author Manuscripts

Europe PMC Funders Author Manuscripts

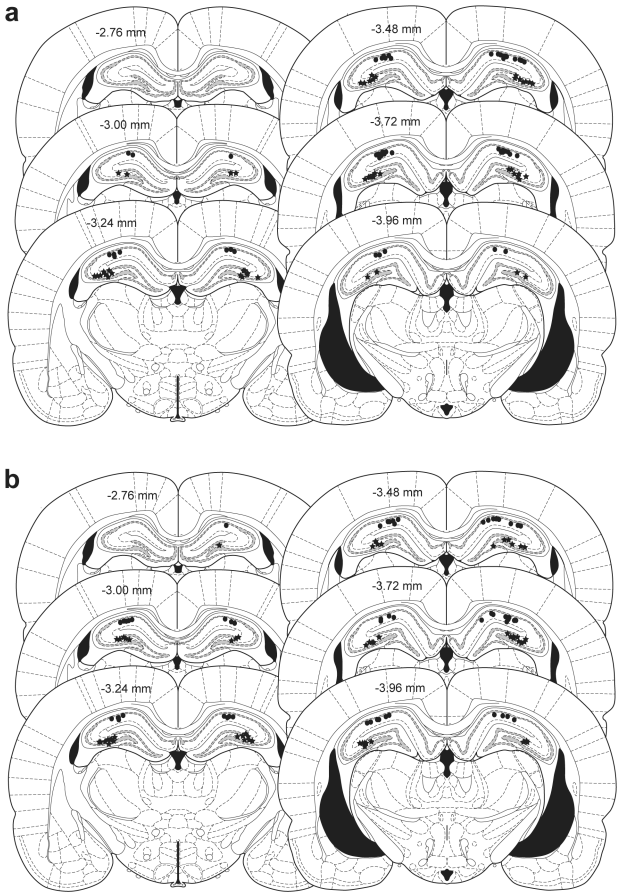

Figure 6. Depth profiles during electrode implantation

(**a & b**) Changes in peak fEPSP amplitude elicited by ipsilateral (**a**) and contralateral (**b**) CA3 stimulation as a recording electrode is lowered into the hippocampus of a single rat; sample fEPSPs are shown at different depths (scale bar: vertical = 3 mV; horizontal = 5 ms); note the large negative-going responses elicited in the stratum radiatum by both ipsilateral and contralateral stimulation. (**c**) A schematic illustration of the locations of recording and stimulating electrode (see below) tracks in the same rat, based on the coronal section in which the location of the stimulating electrodes was most clearly visible. (**d & e**) Examples of fEPSP amplitude depth profiles recorded in the same animal as a stimulating electrode was lowered ipsilaterally (**d**) or contralaterally (**e**) relative to a stationary recording electrode in the stratum radiatum. Note the large negative-going responses elicited by both ipsilateral and contralateral stimulation of CA1 and CA3; sample fEPSPs are shown (scale bar: vertical = 3 mV; horizontal = 5 ms).

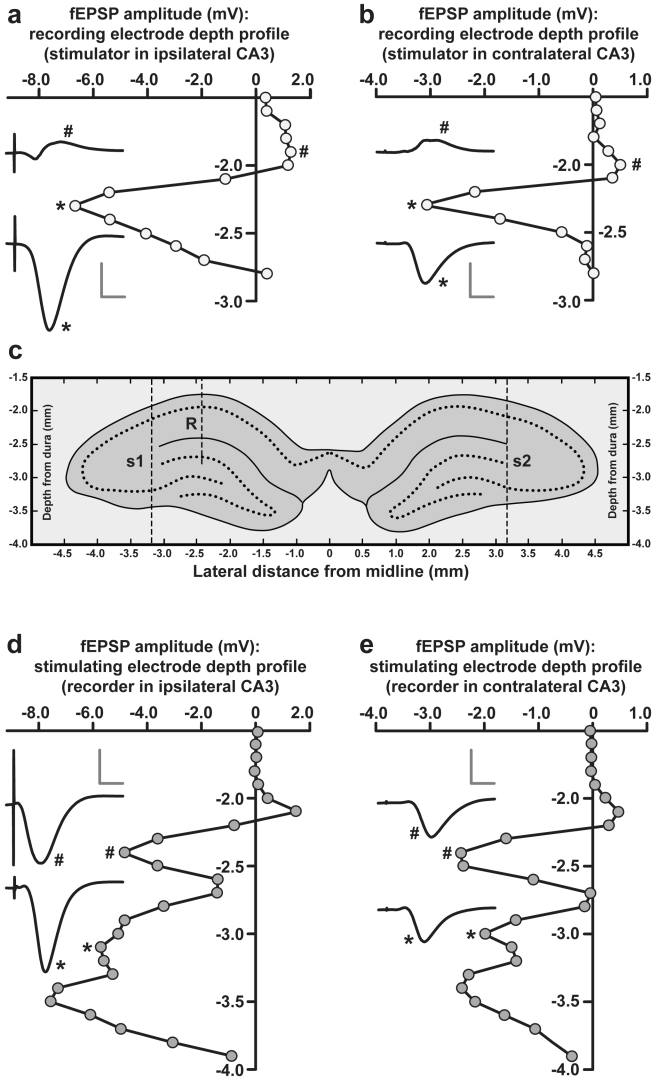

Figure 7. Histology

Locations of the marking lesions made via all stimulating (filled stars) and recording electrodes (filled circles) used in Experiment 1 (**a**), Experiment 2 (**b**), and Experiment 3 (**c**); the locations of infusion cannulae are indicated by open squares in (**c**). Numbers indicate distance from bregma. Figures are adapted from Paxinos and Watson, 2005[60].

Europe PMC Funders Author Manuscripts

Table 1

Baseline parameters

The left-hand panels show mean baseline fEPSP slope values over the first hour of recording in experiments 1-3, the middle panels show stimulation intensities, and the right-hand panels show mean paired-pulse facilitation (PPF) following alternate stimulation of $s2_c$ followed by $s1_i$ at an interval of 50 ms for experiments 1 & 2. PPF was not assessed in experiment 3. There were no significant group differences in baseline fEPSP slope or stimulation intensity, although baseline fEPSPs in $s2_i$ were typically slightly larger than those in $s1_c$ (see main text).

	bas eline fEPSP slope (mV/ms)		**stimulation intensity (μA)**		**PPF %**
Experiment 1	**s1i**	**s2 c**	**s1 i**	**s2c**	**s2c -s1i**
aCSF + strong	−0.99 ± 0.17	−0.79 ± 0.11	458 ± 27	383 ± 56	99.2 ± 2.3
ANI + strong	−1.12 ± 0.23	−0.61 ± 0.10	421 ± 41	429 ± 47	100.9 ± 2.3
strong be fore strong + ANI	−1.32 ± 0.12	−0.81 ± 0.10	4 33 ± 36	472 ± 28	99.9 ± 2.9
Experiment 2	**s1i**	**s2c**	**s1i**	**s2c**	**s2c -s1i**
strong only	−1.15 ± 0.11	−1.05 ± 0.13	414 ± 46	379 ± 4 7	100.4 ± 2.6
weak only	−1.39 ± 0.15	−0.69 ± 0.10	427 ± 31	386 ± 35	98.7 ± 1.5
weak before strong	−1.32 ± 0.24	−0.67 ± 0.16	382 ± 33	432 ± 31	101.8 ± 0.7
Experiment 3	**s1i**	**s2c**	**s1i**	**s2c**	**s2c -s1i**
aCSF	−0.68 ± 0.06	−0.77 ± 0.07	291 ± 23	364 ± 54	---
SCH23390	−0.73 ± 0.07	−0.79 ± 0.09	304 ± 35	324 ± 46	---